Novel Protein Interactions with Endoglin and Activin Receptor-like Kinase 1: Potential Role in Vascular Networks*⑤

Guoxiong Xu‡§¶‖‖‖, Miriam Barrios-Rodiles‖‖‖, Mirjana Jerkic§¶, Andrei L. Turinsky§,
Robert Nadon‡‡, Sonia Vera§, Despina Voulgaraki§¶, Jeffrey L. Wrana**,
Mourad Toporsian§‖§§¶¶, and Michelle Letarte§¶‖¶¶**

Endoglin and activin receptor-like kinase 1 are specialized transforming growth factor-beta (TGF-β) superfamily receptors, primarily expressed in endothelial cells. Mutations in the corresponding *ENG* or *ACVRL1* genes lead to hereditary hemorrhagic telangiectasia (HHT1 and HHT2 respectively). To discover proteins interacting with endoglin, ACVRL1 and TGF-β receptor type 2 and involved in TGF-β signaling, we applied LUMIER, a high-throughput mammalian interactome mapping technology. Using stringent criteria, we identified 181 novel unique and shared interactions with ACVRL1, TGF-β receptor type 2, and endoglin, defining potential novel important vascular networks. In particular, the regulatory subunit B-beta of the protein phosphatase PP2A (PPP2R2B) interacted with all three receptors. Interestingly, the *PPP2R2B* gene lies in an interval in linkage disequilibrium with HHT3, for which the gene remains unidentified. We show that PPP2R2B protein interacts with the ACVRL1/TGFBR2/endoglin complex and recruits PP2A to nitric oxide synthase 3 (NOS3). Endoglin overexpression in endothelial cells inhibits the association of PPP2R2B with NOS3, whereas endoglin-deficient cells show enhanced PP2A-NOS3 interaction and lower levels of endogenous NOS3 Serine 1177 phosphorylation. Our data suggest that endoglin regulates NOS3 activation status by regulating PPP2R2B access to NOS3, and that PPP2R2B might be the HHT3 gene. Furthermore, endoglin and ACVRL1 contribute to several novel networks, including TGF-β dependent and independent ones, critical for vascular function and potentially defective in HHT. *Molecular & Cellular Proteomics* 13: 10.1074/mcp.M113.033464, 489–502, 2014.

Transforming growth factor-β (TGF-β)[1] superfamily ligands, including TGF-βs, activins and bone morphogenic proteins (BMPs), regulate several pathways essential for vascular development and function (1). Responses to these ligands are controlled by type I and II serine kinase receptors, coreceptors and signaling SMAD intermediates. Endothelial cells express the coreceptor, endoglin, and the specialized type I receptor, ACVRL1 (activin receptor-like kinase 1 or ALK1); both molecules are critical for regulation of angiogenesis and vasomotor function by TGF-β superfamily ligands (2, 3).

Mutations in *ENG* and *ACVRL1* genes lead to hereditary hemorrhagic telangiectasia (HHT), types 1 and 2, respectively (4). HHT affects 1 in 5000–8000 people worldwide and is characterized by arteriovenous malformations (AVMs) in mul-

tiple organs, potentially leading to severe hemorrhages and strokes (4). Haploinsufficiency is the underlying cause of HHT, indicating that reduced levels of functional endoglin or ACVRL1 (ALK1) proteins predispose to endothelial dysfunction and AVMs (5). Although the mechanisms responsible for AVMs remain unclear, the elucidation of how members of the TGF-β superfamily and their molecular networks regulate vascular integrity is vital for future treatments of HHT.

We have demonstrated that endoglin interacts with endothelial nitric oxide synthase (NOS3 or eNOS) and regulates its activation (2). NOS3 is a Ca^{+2} and calmodulin-regulated enzyme that produces NO● in response to humoral and mechanical stimuli via dynamic interactions with various allosteric regulators such as heat shock protein 90 (HSP90). NOS3 is also regulated by dynamic changes in its phosphorylation status. For example, effects of the vascular endothelial growth factor (VEGF) on angiogenesis, vascular permeability and vasomotor tone are mediated in part through Akt-dependent phosphorylation of NOS3 Ser1177 and by increased NOS3-HSP90 association (6). Although phosphorylation of NOS3 Ser1177 is indicative of agonist-induced activation, it is preceded by dephosphorylation at Thr495. TGF-β1 and -β3 but not -β2 responses can sensitize NOS3 for activation by inducing dephosphorylation at Thr495, and therefore contribute to NOS3 activation and NO-dependent vasorelaxation (7). Endoglin regulates TGF-β1 and -β3 but not -β2 responses, and is required for their induction of NOS3 Thr495 dephosphorylation (7, 8).

In the vascular endothelium of HHT patients and in *Eng* and *Alk1* heterozygous mice, impaired association of NOS3 with HSP90 renders the enzyme uncoupled, causing production of superoxide (●O_2^-) instead of NO● (2, 3, 9) and leading to endothelial damage. Interestingly, TGF-β1 and -β3 do not induce phosphorylation at NOS3 Ser1177, yet NOS3 activation in response to TGF-β1 is abolished in endoglin-deficient cells, impairing vasomotor function (3). ACVRL1 (or ALK1) also interacts with NOS3, and its reduced levels in endothelial cells similarly cause NOS3-derived oxidative stress (3, 9).

In view of the crucial roles of endoglin and ACVRL1 in the development and maintenance of the normal vasculature and the definite contribution of their mutated state to HHT, we used the LUMIER high-throughput technology (10) to identify novel protein interactions and molecular networks for these predominantly endothelial receptors. We included TGFBR2 to further define TGF-β protein networks potentially important for vascular function, and attempt to distinguish the TGF-β networks from those associated with BMP9/BMP10 and mediated by ACVRL1 in a complex with BMPR2 and endoglin (11, 12).

One of identified proteins interacting with all three receptors was protein phosphatase 2A (PP2A), implicated in multiple pathways. PP2A is a holoenzyme with one structural subunit (PPP2R1A or PPP2R1B) associated with one catalytic subunit (PPP2CA or PPP2CB) and one of 19 regulatory B subunits,

the latter conferring specificity to the enzyme by recruiting interacting proteins (13, 14). Of interest, PP2A interacts with NOS3 to regulate Ser1177 phosphorylation and NO● production (15). However, the mechanisms governing recruitment of PP2A to NOS3 and the contribution of TGF-β/BMP receptor complexes are unknown. Recently, the human *PPP2R2B* gene coding for PPP2R2B protein (also known as PP2A-Bβ regulatory subunit) was mapped to chromosome 5q31-q32, in an interval in linkage disequilibrium with the HHT3 locus (16, 17). We now report that PPP2R2B interacts with the ACVRL1/ TGFBR2/endoglin complex and that endoglin governs NOS3 phosphorylation and activation status by hindering PP2A access to NOS3 via the PPP2R2B subunit. Loss of endoglin leads to constitutive reduction in NOS3 phosphorylation and likely to changes in several networks with consequent endothelial dysfunction.

EXPERIMENTAL PROCEDURES

Cell Culture—HEK-293T cells obtained from ATCC and cultured in Dulbecco's Modified Eagle Medium with 100 IU/ml penicillin, 100 μg/ml streptomycin, and 10% FCS (Invitrogen, Carlsbad, CA). Mouse endothelial cells derived from day 9 *Endoglin* null (*Eng*$^{-/-}$) and littermate *Eng*$^{+/+}$ embryos, were maintained in MCDB131 medium as described (18). Bovine aortic endothelial cells kindly provided by Dr. Calvin Vary (Maine Medical Center, USA) were maintained in M199 medium with 10% fetal calf serum (FCS), plus the supplements mentioned above for mouse endothelial cells.

LUMIER Screen—Novel signaling networks associated with TGF-β superfamily receptors, were identified by LUMIER (10). HEK-293T cells were cotransfected in 96-well plates with 640 Flag-tagged cDNA plasmid preys and a Renilla luciferase-tagged receptor bait (ACVRL1, ENG, and TGFBR2 respectively). The 640 proteins used as preys were originally cloned as described (10). The majority of cDNAs were selected from the mouse FANTOM library (19) as open reading frames that contained at least one domain of interest in signal transduction, such as kinase, phosphatase, Ras, WD40, LIM, PDZ, Arm, and SH2. The tagged receptor bait in complex with a Flag-tagged prey was detected as light emission by the immunoprecipitates. Screening was performed in four independent experiments for ACVRL1 and in two independent experiments for both ENG and TGFBR2.

Expression Constructs and Transfection—Most expression constructs were generated as described (10, 20). All plasmids were confirmed by restriction enzyme digestion and sequencing (Sequencing Facility, The Centre for Applied Genomics, The Hospital for Sick Children, University of Toronto). HEK-293T cells were seeded in six-well plates at 2.5×10^5 cells/well and transfected with 1 μg plasmid DNA (unless otherwise specified) using FuGENE6 (Roche).

Immunoprecipitation and Western Blot—Cells were lysed with TNE buffer (0.05 M Tris/HCl, pH7.4, 0.1 M NaCl, 1 mM EDTA) supplemented with 0.5% Triton X-100, 0.01 M $Na_4P_2O_7$, 0.025 M NaF, and 1 mM Na_3VO_4 plus proteases inhibitors (Roche), lysates were centrifuged at $10,000 \times g$ for 15 min and precleared using Protein G or A Sepharose beads (GE Healthcare). After protein estimation, 700–800 μg total protein lysate was used for immunoprecipitation (IP), whereas 20 μg was reserved for each Western blot (WB). Generally, 1 μg/sample of primary antibody was added to the precleared lysate and incubated for 16 h, followed by IP with 25 μl of Protein G or A Sepharose bead slurry for 45 min at 4 °C, and 4 washes in TNE buffer + 0.1% Triton X-100 before elution in sample gel buffer at 95 °C for 5 min. Equal protein amounts were fractionated on 4–12% gradient NuPAGE gels (Invitrogen) and transferred to a PVDF membrane (Immobilon-P, Mil-

lipore Corp, Bedford, MA). After blocking with 5% milk in Tris-buffered saline pH 7.4, 0.1% Tween 20, the blot was incubated with primary antibody for 2 or 16 h and followed by a secondary antibody conjugated with horseradish peroxidase (HRP) for 1 h. Signals were detected using an ECL-Plus kit (Amersham Biosciences).

The following antibodies were used: mouse anti-Flag (M2) (Sigma); rabbit anti-PP2A/B$\alpha\beta$ (Cell Signaling; reacting with PPP2R2A and PPP2R2B); rabbit anti-PP2A/Bβ (Stratagene; reacting with PPP2R2B); mouse anti-PP2A/C (Upstate; reacting with both PP2A catalytic subunits), mouse anti-NOS3 (BD Transduction), rabbit anti-phospho-NOS3 (Ser 1177), rabbit anti-HA (Y-11) and polyclonal anti-human endoglin (H-300) (Santa Cruz, Santa Cruz, CA); rat anti-mouse endoglin (MJ7/18) (Southern Biotech); donkey anti-rabbit IgG HRP, sheep anti-mouse IgG HRP and goat anti-rat IgG HRP (GE Healthcare).

Bioinformatics and Data Analysis—Data were analyzed by three independent methods to generate a list of potential candidate preys interacting with the receptor baits. The LUMIER intensity ratio (LIR) was calculated as X/μ_n, where X is the raw luminescence value in a given well, and μ_n the mean of negative controls within a plate (10). These were ranked from high to low and those greater than five, were retained. The Robust Z score (RZ) (21), was measured by the formula (X - Med)/MAD, where Med is the median of all values within a plate and MAD, the absolute deviation from the median (21). An RZ score >3 indicated a signal at least threefold above the median of all values within a plate. The 10% Trimmed Polish (TP10) method (22) was evaluated on a plate-by-plate basis to remove column and row effects using a 10% trimmed polish before calculating the mean for the polish. All TP10 values were ranked from high to low and the top 20% of proteins were retained. The top 20% TP10 scores were 1.02 for ACVRL1, 1.66 for ENG, and 1.10 for TGFBR2 (as indicated in supplemental Table S1).

A web-based Ingenuity® Pathway Analysis was used to determine biological processes and functions for selected proteins and Cytoscape was applied to generate potential protein–protein networks. Comparison of experimentally determined interactions that passed our stringent analysis criteria to those of literature-curated protein–protein interaction data were performed as described in supplemental Material. The literature-curated datasets from iRefWeb and BioGRID are publically available from the corresponding resource websites.

Comparison of Experimentally Determined to Literature-curated Protein–Protein Interactions—Literature-curated protein-protein interaction data were retrieved from the iRefWeb resource (23). iRefWeb contains a large collection of protein interactions consolidated from 14 major public databases, including BioGRID, MINT, IntAct, DIP, HPRD, and others. The data were then complemented by the most current release 3.2.100 of the BioGRID resource (24). In addition we manually extracted relevant interactions from several publications, which, to our knowledge, have not yet been annotated by public databases (2, 3, 25, 26).

Interactions data from Human, Mouse and Rat were consolidated into a single set using homology information from Ensembl (27) and Inparanoid (28) resources. Because the human interaction network is the largest and most complete of the three interactomes, we used human proteins for representing network nodes in the comparative analysis with literature-curated interactions. Several nodes for which human homologs were unavailable were represented using mouse gene names, such as *Rasl2-9* and *Gmcl1l*.

Direct interactions were identified using a combination of PSI-MI ontology codes, extracted from the interaction annotations. First, we collected records annotated with the interaction type MI:0407 "direct Interaction" or its descendants. Second, we also collected records detected using the following experimental methods: MI:0090 "protein complementation assay," MI:0114 "x-ray crystallography," MI:0415 "enzymatic study," MI:0047 "far Western blotting," and MI:0055 "fluo-

rescent resonance energy transfer." All other records—including many with missing annotation codes—were considered indirect protein associations.

Statistical Analysis—Data from coIP/WB experiments (Fig. 6), are expressed as ratios and therefore were converted to $\log_2$ before 2 × 3 ANOVA analysis. In cases in which interactions were expected from the literature, a *t* test with Welch correction for unequal variances was applied. $p < 0.05$ was considered significant.

RESULTS

Identification of Proteins Interacting with ACVRL1, Endoglin and TGFBR2 by LUMIER Assay—Using the LUMIER assay (10, 29), we identified proteins interacting with ACVRL1 (ALK1), ENG (endoglin), and TGFBR2 (TGF-β receptor 2) and implicated in the regulation of vascular functions. A stringent list of potential interactors was generated by three independent methods. Luminescence intensity ratio (LIR; the ratio of bound luminescence to background binding to negative controls) > 5 and that displayed a RZ score (21) > 3 (implying a signal 3 standard deviations above the median), were further filtered by the 10% Trim Polish method (22) to eliminate plate-effects (supplemental Table S1 lists interaction scores for preys and baits). This table also indicates five proteins shown previously to interact with Renilla luciferase itself (10) and therefore considered false-positive. The LIR, RZ, and TP10 methods were relatively well correlated ($r = 0.8$) (Fig. 1*A*) and preys matching all three criteria yielded 87, 76, and 28 interactions with ACVRL1, TGFBR2, and endoglin respectively. Interactions with the three receptors were next visualized using a network graph (Fig. 1*B*) and Venn diagram (Fig. 1*C*).

Of the 191 interactions identified, 34 were for preys associated with ACVRL1 and TGFBR2 and 13 were for preys interacting with all three receptors. Table II reports the ranking order of the RZ scores for these shared interactions. Of these 13 preys, four of them (PLEKHB1, FBXO3, PAK1, and BCR) were previously shown to interact with other receptors including TGBR1, ACVR1, and BMPR1B in a LUMIER screen (10). However, ARL4D, PREB, EIF2AK4, RALGPS2, WDR13, and importantly, PPP2R2B, did not bind to ACVR1 or BMPR1B in the previous study, highlighting the specificity of the interactions detected by LUMIER. Furthermore, these 13 proteins also displayed differential interactions when tested against core members of the Wnt pathway (29), although there were no receptors in the set of baits used in the Wnt pathway LUMIER screens.

Thus, 47 newly identified interactors may form complexes with TGFBR2 and the endothelial specific type I receptor ACVRL1, and potentially mediate TGF-β effects in the endothelium. The 34 proteins interacting with ACVRL1 alone and the six proteins interacting with ACVRL1 and ENG may be involved in BMP9 pathways, as opposed to TGF-β pathways. The 21 proteins binding TGFBR2 alone, and the eight proteins binding endoglin and TGFBR2 may be ACVRL1-independent, acting via TGFBR1 (ALK5).

FIG. 1. **Identification of proteins interacting with ACVRL1, endoglin and TGFBR2 receptors of the TGF-β superfamily.** Interactions of 640 Flag-tagged preys with the receptor baits were measured by the LUMIER screen. *A*, Scatter plots showing good correspondence among the scores obtained by three different methods: LIR, RZ, and TP10 as described in Materials and Methods. For each of the three panels (ACVRL1, ENG, and TGFBR2), density plots for each of the methods are shown on the diagonals; bottom left off-diagonal graphs show scatterplots between variable pairs indicated in the corresponding *x*- and *y* axis labels; correlations between variable pairs indicated in the corresponding *x*- and *y* axis labels are shown at the top right. The panels corresponding to the scores determined by the same method on each axis (*e.g.* LIR *versus* LIR) simply represent the empirical distribution of the scores derived from the content of the screen by that method. Data were normalized and are shown as replicate means of repeated experiments. Each experiment contained duplicates of each prey and two different experiments were done for endoglin and TGFBR2 and four for ACVRL1. *B*, Network of potential interactions between preys and the TGF-β receptors generated using Cytoscape. Flag-tagged preys with LIR >5, RZ >3 and classified in the top 20% for TP10, were considered strong candidates for positive interaction and are shown here. *C*, Venn Diagram representing the number of preys meeting the three stringency criteria for interactions with ACVRL1, TGFBR2, and endoglin respectively.

TABLE I

ACVRL1, endoglin and TGFBR2 interactions with phosphatase subunits detected in the LUMIER screen

Protein and human gene #	Description	ACVRL1 scores[a]			ENG scores			TGFBR2 scores		
		RZ	LIR	TP10	RZ	LIR	TP10	RZ	LIR	TP10
PP2A Regulatory subunits										
PPP2R2B 5521	Subunit B, B-β isoform, 55kDa	**5.4**	**39.4**	**2.5**	**4.5**	**5.3**	**2.2**	**3.5**	**8.6**	**1.2**
PPP2R2D 55844	Subunit B, B-δ isoform, 55kDa	0.6	**12.1**	−0.5	0.3	3.7	1.5	1.2	**5.1**	0.4
PPP2R5A 5525	Subunit B, B'-α isoform, 56kDa	1.2	**8.2**	0.8	0.6	1.4	0.3	1.7	2.6	1.1
PPP2R5B 5526	Subunit B, B'-β isoform, 56kDa	−1.0	2.0	−0.2	−1.1	0.9	−0.3	−1.0	0.9	−0.3
PPP2R5C 5527	Subunit B, B'-γ isoform, 56kDa	−0.3	4.1	−1.6	−0.9	1.0	−1.1	0.1	1.6	−1.2
PPP2R5D 5528	Subunit B, B'-δ isoform, 56kDa	1.8	**10.1**	−0.3	−0.3	1.1	−0.8	0.5	1.9	−0.8
PP2A Structural subunit										
PPP2R1B 5519	Subunit A, PR65-β isoform, 65kDa	**5.5**	**19.6**	**1.9**	2.4	1.9	0.8	**4.6**	4.3	**2.2**
PP2A Catalytic subunits										
PPP2CA 5515	Subunit C, -α isoform, 36kDa	**3.0**	**14.7**	1.2	0.9	1.8	0.5	0.6	3.5	0.1
PPP2CB 5516	Subunit C, -β isoform, 36kDa	**7.6**	**25.2**	**2.9**	**3.4**	1.9	1.2	**3.1**	3.4	1.9
Other PP subunits										
PPP3CC 5533	PPP3, PP2B catalytic subunit γ, or calcineurin	0.8	**16.4**	0.7	−0.1	1.7	0.8	0.8	**5.6**	1.0
PPP6C 5537	PP6 Catalytic subunit	2.8	**14.1**	−0.0	1.1	2.3	0.3	2.94	**6.8**	0.3

[a] RZ, LIR, and TP10 scores were calculated as described in Methods, taken from supplementary Table S1 where scores for all bait–prey interactions are shown, and rounded off to one decimal. Those indicated in bold were above the cutoff line for the stringent criteria selected for the individual scores.

TABLE II

Ranking order based on RZ scores for preys interacting with all three receptor baits. The ranking order for each bait–prey interaction was based on the mean RZ score, indicated in parentheses. Other scores are listed in supplemental Table S1

Interacting preys	Ranking order and (RZ score)		
	ENG	TGFBR2	ACVRL1
TGFBR1	1 (37.9)	8 (6.0)	4 (9.6)
PLEKHB1	2 (27.8)	9 (5.8)	2 (14.6)
RALGPS2	3 (18.7)	2 (9.4)	1 (15.6)
FBXL12	4 (16.4)	5 (8.1)	9 (5.6)
RAD23A	5 (14.5)	11 (3.7)	12 (4.0)
FBXO3	6 (13.3)	10 (5.4)	5 (8.0)
ARL4D	7 (10.7)	1 (21.0)	3 (10.1)
BCR	8 (9.5)	7 (6.6)	11 (4.4)
PAK1	9 (9.4)	13 (3.2)	6 (6.9)
PREB	10 (5.8)	6 (6.7)	8 (6.0)
EIF2AK4	11 (5.0)	3 (9.3)	7 (6.4)
PPP2R2B	12 (4.5)	12 (3.5)	10 (5.4)
WDR13	13 (3.7)	4 (9.1)	13 (3.9)

We next validated a series of interactions by transient cotransfection in HEK-293T cells (supplemental Figs. S1 and S2). PAK1, a serine kinase that links RhoGTPases to the cytoskeleton and FBXL12, a component of the SCF ubiquitin-ligase complex, were previously shown to interact with TGFBR1 (10). We independently confirmed by LUMIER and IP/WB that PAK1 and FBXL12 interact with ACVRL1, endoglin, and TGFBR2 (supplemental Fig. S1*A*, S1*B,* and S1*C*). IRF7, RIT1, ARL4D, WWOX, IKBKE, and RAC2 were validated as interactors of TGFBR2 (supplemental Fig. S1*D*). RAC2 association detected by IP/WB was slightly below the cut-off for TGFBR2 and endoglin, yet above that for ACVRL1, confirming the high stringency of our criteria and suggesting that even interactions below the cutoff point might be significant.

Novel Protein Interactions for Endoglin, ACVRL1, and TGFBR2—A review of the protein-interaction data sets curated from the literature revealed that of the 191 pairs detected in the current study, only 10 were previously reported. Four have been unambiguously curated as direct physical interactions (by the BioGRID and InnateDB teams): ENG/TGFBR1 (30); TGFBR1/TGFBR2 (31, 32); AP2B1/TGFBR2 (33); and PAK1/TGFBR2 (10). The other six pairs have appeared as part of known protein complexes or in literature-curated interactions with incomplete annotations (TGFBR2 with MAP3K7, OXSR1, PARD6A, PPP1CA, and SMURF1; and ACVRL1 with TGFBR1). The remaining 181 pairs detected by LUMIER in the current study represent novel potential interactions. Data analysis also revealed 28 interactions among literature-curated pairs that were tested in the LUMIER screen but did not pass our stringent filters. Four of these were previously annotated as direct pairwise interactions, three of which were confirmed by co-IP studies but had low scores in our screen: ENG/AKT1 (26); ENG/TRIP6 (34); and TGFBR2/STRAP (35).

Novel interactions identified in our study were then combined with literature-curated data to yield an extensive network of proteins centered on ACVRL1 and endoglin hubs (Fig. 2). To reduce complexity, TGF-β superfamily ligands and receptors other than endoglin and ACVRL1 were omitted. Using the GO molecular function categories, preys were grouped into an ATP binding hub of 21 kinases, a GTP binding group of 19 small GTPases and related proteins, an ubiquitin-protein ligase activity group, and a phosphatase group including PP2A subunits, NOS3, and the HSP90 chaperones.

To clarify how the novel receptor networks relate to each other and to those of TGFBR1 (ALK5), we compared the newly identified and literature-curated interactions for each pair of receptors. ACVRL1 and TGFBR2 share multiple interactors including 47 novel ones, but also have unique partners (Fig. 3*A*) that include 40 ACVRL1-specific interactions. Compari-
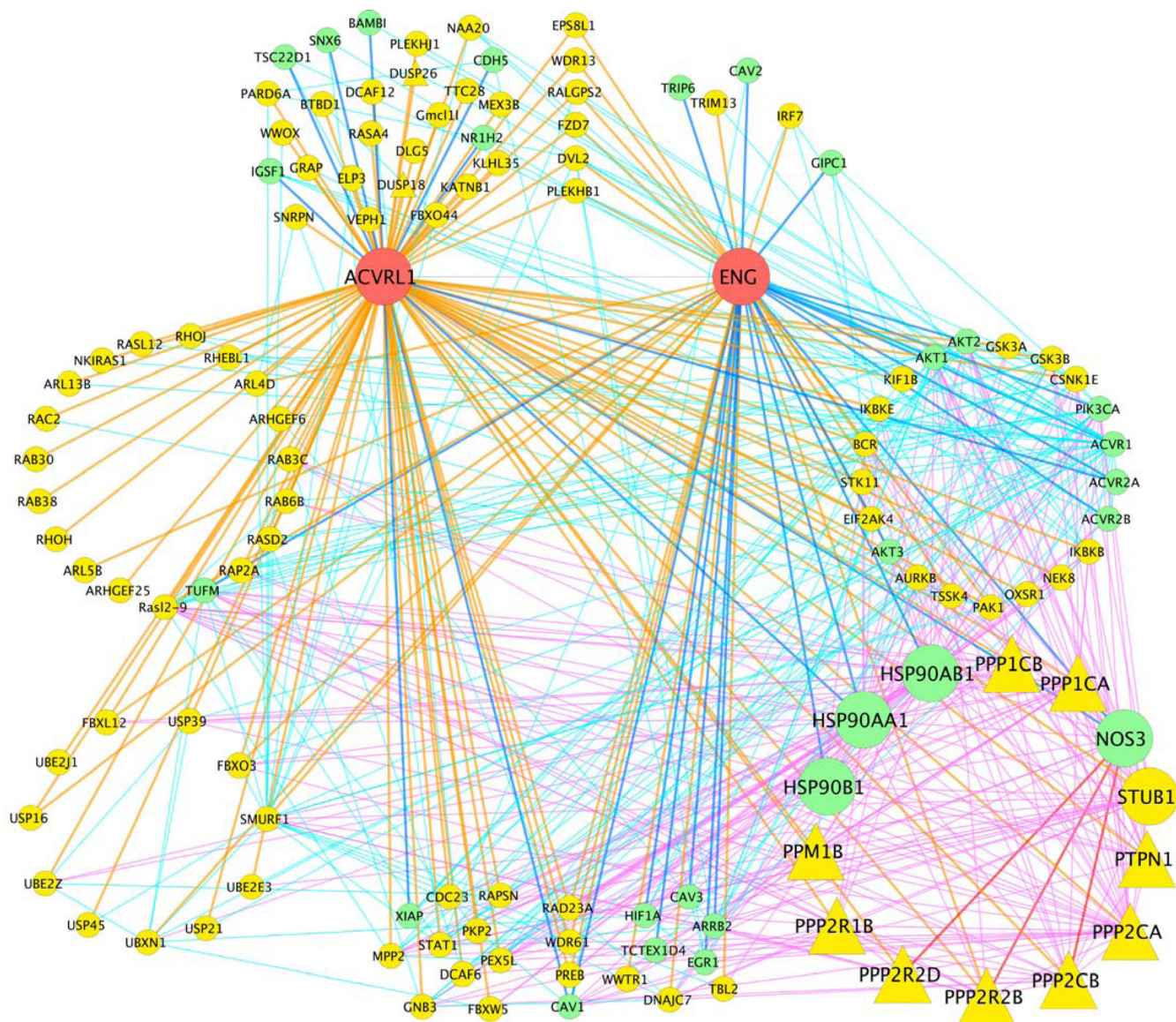
Fig. 2. **Network of interactions between ACVRL1, endoglin and the newly identified partners, based on literature-curated protein interaction data.** The bait nodes ACVRL1 and endoglin are in pink and the novel LUMIER-detected interacting preys identified in this study are represented by orange nodes and edges. Interactions from the literature are shown as green nodes and blue edges, light blue and dark blue representing prey-prey and bait-prey interactions respectively. Phosphatases are shown as triangles. Four hubs regrouping proteins according to their GO term functional category are illustrated: ATP binding proteins; phosphatases (PP2A and associated proteins); ubiquitin-protein ligase activity; GTP binding proteins. The light pink edges represent the PP2A network whereas the dark pink edges highlight the PP2A subunit interactions with NOS3 shown by IP/WB in the current study. The numerous interactions for TGFBR1 (ALK5), TGFBR2 and TGFBR3 (betaglycan) were omitted from this diagram to focus on potential ACVRL1 and endoglin networks of endothelial cells.

son of endoglin and TGFBR2 networks similarly revealed 21 novel and seven known interactors for these two receptors; it also showed many endoglin-specific interactions, consistent with the ability of endoglin to mediate activin and BMP pathways (Fig. 3B). Finally, a comparison of ACVRL1 and endoglin networks highlights that each have independent networks in addition to sharing multiple interactors (19 novel, eight known) (supplemental Fig. S3). This difference in ACVRL1 and endoglin networks might explain some of the clinical differences between HHT1 and HHT2.

We also compared ACVRL1 (ALK1) and TGFBR1 (ALK5) newly defined interactions, which revealed many common networks (supplemental Fig. S4), in agreement with the observations that ALK5 is required in the receptor complex to mediate ALK1-dependent TGF-β1 responses in endothelial cells (36). Also highlighted in supplemental Fig. S4 are many novel ACVRL1-specific partners likely involved in BMP9 signaling. supplemental Fig. S5 shows that endoglin and TGFBR1 have common and mutually exclusive networks, as endoglin is known to mediate non-TGF-β dependent path-
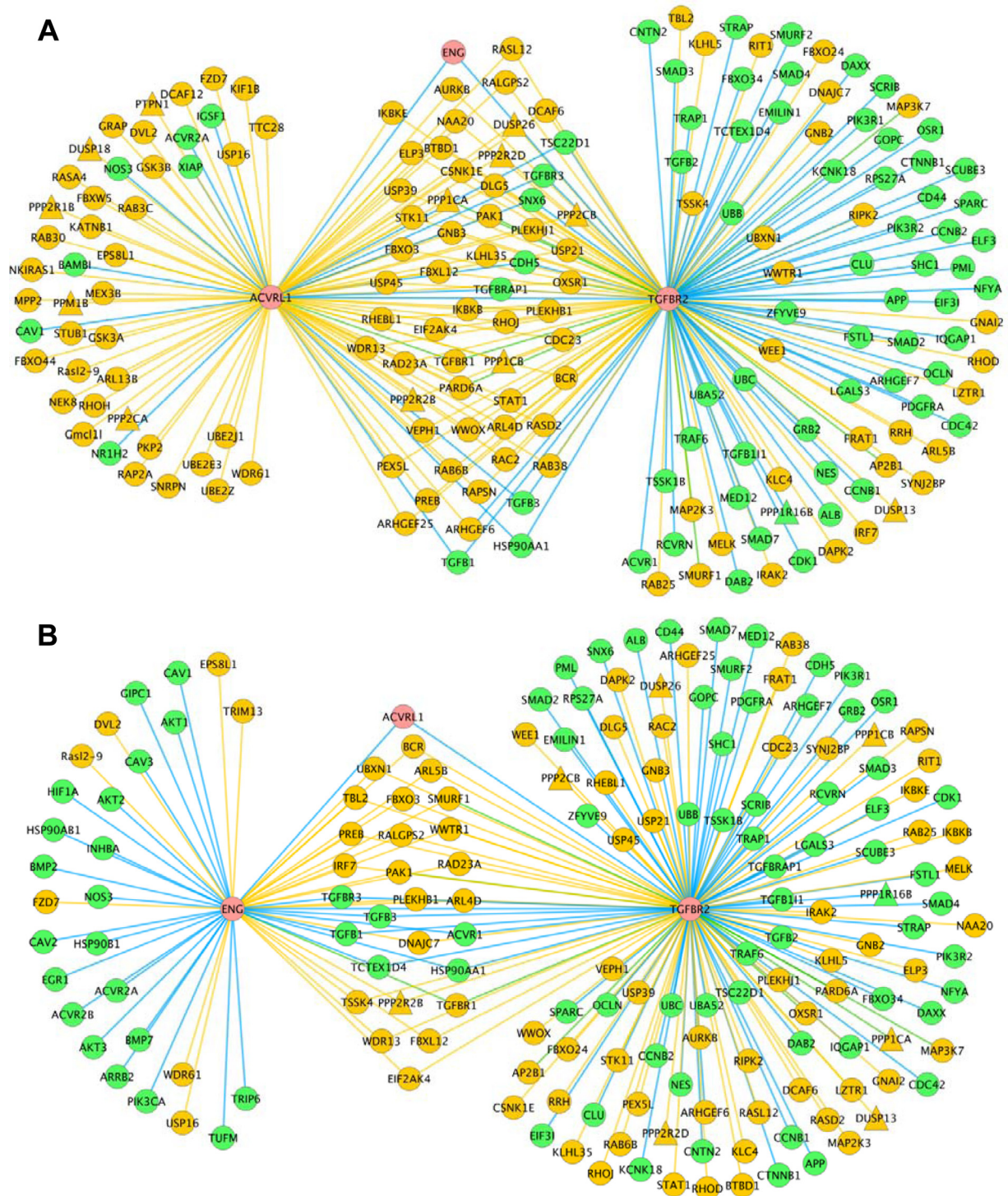
FIG. 3. **TGFBR2 networks of protein interactions compared with those of ACVRL1 and endoglin.** The baits are in pink, the novel interacting nodes and edges are in orange whereas the literature-derived interacting nodes and edges are in green; light blue and dark blue represent prey-prey and bait-prey interactions respectively. *A*, Shared networks between TGFBR2 and ACVRL1. *B*, Shared networks between TGFBR2 and endoglin.

ways, but activin or BMP dependent. TGFBR2 and TGFBR1 shared networks were expectedly large as these two receptors form a heteromeric complex to mediate TGF-β effects in many cell types (supplemental Fig. S6). In summary, our studies show that endoglin and ALK1 share multiple potential partners, including those mediating TGF-β signals in association with TRGBR2 and ALK5. Our findings confirm the numerous studies outlining the contribution of endoglin and
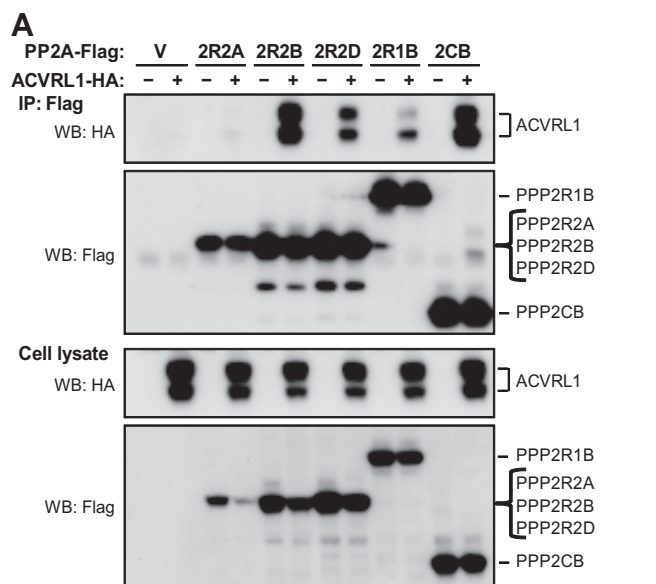
FIG. 4. **Interaction of PP2A subunits with ACVRL1, TGFBR2 and endoglin.** HEK-293T cells were cotransfected with pCMV5 control vector (V), different Flag-tagged PP2A subunit constructs (0.4 μg DNA) and the HA-tagged receptors (1.6 μg DNA) indicated. Protein lysates were subjected to immunoprecipitation (IP) with an antibody to the Flag tag, followed by Western blot (WB) with anti-HA for ACVRL1 (*A, C*), TGFBR2 (*B, D*) and endoglin (*C, D*). Representative IP and WB show that PPP2R2B interacted with ACVRL1 ($n = 6$), endoglin ($n = 4$), and TGFBR2 ($n = 3$).
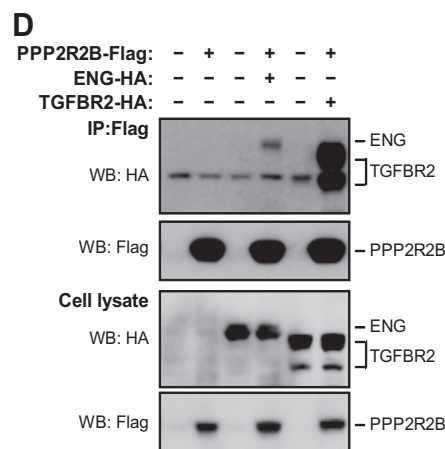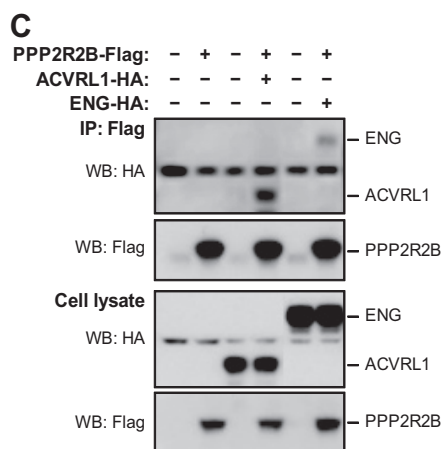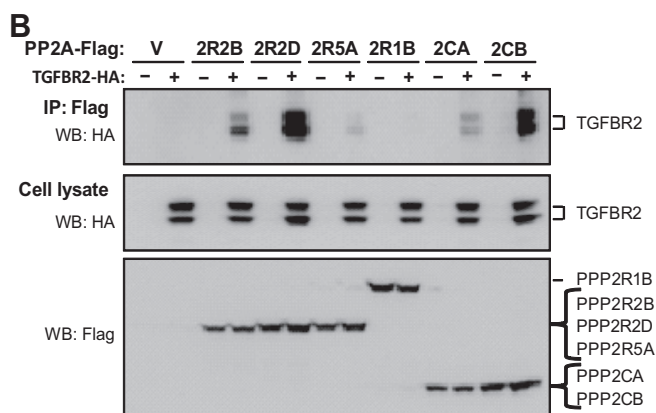
ALK1 to TGF-β1 and -β3 mediated pathways in endothelial cells.

PPP2R2B Interacts with ACVRL1, TGFBR2, and Endoglin— One of the subnetworks identified by LUMIER was that of the protein phosphatase 2A (PP2A; Fig. 2, enlarged hubs). Of the regulatory PP2A subunits tested, PPP2R2B was the only one that passed our stringent data analysis criteria for all of the three baits, ACVRL1, endoglin, and TGFBR2, whereas the scaffolding subunit, PPP2R1B, and the catalytic subunit, PPP2CB were only found associated with ACVRL1 (Table I). This suggested that PPP2R2B is likely the regulatory subunit that recruits the TGF-β receptor complexes to PP2A in endo-
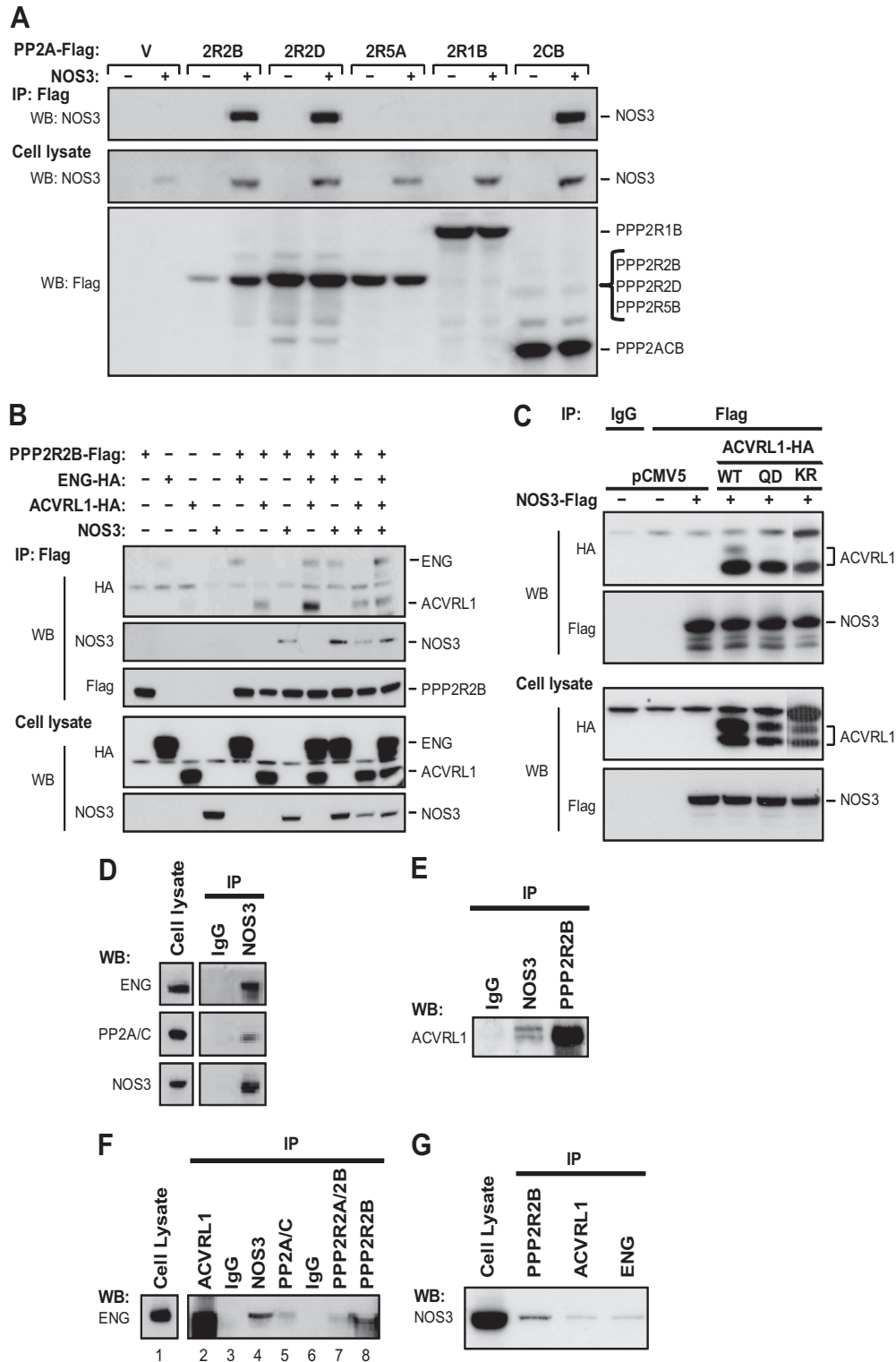
FIG. 5. **PP2A interacts with NOS3 and the TGF-β receptor complex.** *A*, Association of NOS3 with PP2A subunits. HEK-293T cells were cotransfected with pCMV5 control vector (V), different Flag-tagged PP2A subunit constructs and nontagged eNOS (0.4 μg DNA each) as indicated, followed by IP with anti-Flag and WB with anti-eNOS. Interactions between NOS3 and PPP2R2B, PPP2R2D and PPP2CB subunits were observed. *B*, Formation of a complex between PPP2R2B, endoglin, ACVRL1 and NOS3 in HEK-293T cells. Cells were cotransfected with PPP2R2B (0.4 μg), ENG (1.0 μg), ACVRL1 (1.0 μg), and/or NOS3 (0.4 μg) constructs and lysates subjected to IP with anti-Flag (PPP2R2B), followed by WB with anti-HA, anti-NOS3 and anti-Flag. *C*, Constitutively active (QD) and kinase deficient (KR) ACVRL1 interact with NOS3. HEK-293T cells were

thelial cells. Therefore, we further analyzed PPP2R2B and other PP2A subunit interactions with TGF-β superfamily receptors by co-IP in transiently transfected HEK-293T cells. We confirmed the LUMIER screen data for ACVRL1 as it strongly interacted with PPP2R1B, PPP2R2B, and PPP2CB (Fig. 4A). Interestingly, TGFBR1 interacted better with PPP2R2A and PPP2R2D than with PPP2R2B regulatory subunits and associated with PPP2CB and to a lesser degree with PPP2R1B (supplemental Fig. S7A). TGFBR2 analysis also revealed binding to PPP2R2B, PPP2R2D, and PPP2CB (Fig. 4B), but relatively poor interactions with PPP2R5A regulatory and PPP2CA catalytic subunits. Because of the involvement of both endoglin and ACVRL1 in BMP9 signaling, we also tested and found that BMPR2 associates with PPP2R2B and PPP2R2D regulatory subunits (supplemental Fig. S7B). Finally, we compared the various interactions (Fig. 4C, Fig. 4D), and found that the association of PPP2R2B with endoglin is weaker or more transient than those with ACVRL1 and TGFBR2. Interactions of PPP2R2B with ACVRL1, TGFBR2, and endoglin were thus confirmed by co-IP studies in HEK-293T cells and are consistent with the data obtained in the LUMIER screen (Table I and supplemental Table S1).

ACVRL1, Endoglin, PP2A, and NOS3 Form a Complex—We previously demonstrated that endoglin and ACVRL1 interact physically with NOS3 (2, 3), and PP2A is known to dephosphorylate NOS3 (15). In view of the potential involvement of the *PPP2R2B* gene in HHT, we investigated whether PPP2R2B could recruit PP2A to the ACVRL1/TGFBR2/endoglin and NOS3 complexes, to regulate NOS3 activation. Cotransfection experiments in HEK-293T cells using untagged NOS3 and various Flag-tagged PP2A subunits revealed that NOS3 interacts with the regulatory subunits, PPP2R2B and PPP2R2D, and the catalytic subunit PPP2CB. The PPP2R5A regulatory and PPP2R1B structural subunits did not interact with NOS3 (Fig. 5A), underscoring the specificity of the detected interactions.

Cotransfection in HEK-293T cells showed that ACVRL1, endoglin and NOS3 co-IP with PPP2R2B, likely forming a macromolecular complex (Fig. 5B). Wild-type ACVRL1, its constitutively active (QD) or kinase-deficient (KR) mutants all associated with PPP2R2B, suggesting that ACVRL1 interactions were independent of kinase activity (Fig. 5C). To explore the physiological relevance of these interactions, we tested them in mouse endothelial cells. Endoglin and PP2A catalytic subunits interacted with NOS3 (Fig. 5D) whereas ACVRL1 interacted with PPP2R2B and NOS3 (Fig. 5E). Endoglin was immunoprecipitated by antibodies to ACVRL1, NOS3, PP2A catalytic subunit, and PPP2R2B (Fig. 5F). NOS3 was immunoprecipitated with PPP2R2B, ACVRL1, and endoglin (Fig. 5G). These data were reproducible and provide evidence for endogenous complexes comprised of PP2A, NOS3, and the TGF-β receptors in endothelial cells.

Endoglin Regulates PPP2R2B/NO3S Association in Endothelial Cells—To determine how endoglin might modulate PP2A regulation of NOS3, we assessed how ENG overexpression and deficiency affected PPP2R2B/NOS3 interaction in endothelial cells. First we showed that full-length *ENG* (ENG-FL) transfected in bovine endothelial cells decreased PPP2R2B/NOS3 complex formation by 60% ($n = 3$), whereas an *ENG* mutant lacking the cytoplasmic domain (ENG-δCyt), and incapable of binding intracellular PP2A, had little effect (Fig. 6A). We then showed that total NOS3 levels were decreased in $Eng^{-/-}$ cells (Figs. 6B and 6C), as reported previously (2). Nevertheless, the NOS3/PPP2R2B complex relative to total NOS3 was significantly higher in $Eng^{-/-}$ than $Eng^{+/+}$ endothelial cells (2.2-fold increase, $p < 0.005$, Fig. 6B). There was also a relative increase in the NOS3 complex co-IP with an antibody to PP2A catalytic subunit (Fig. 6B). Furthermore, although treatment of $Eng^{+/+}$ cells with TGF-β1 led to increased association of NOS3 with PPP2R2B (2.5-fold increase, $p = 0.07$) and indirectly with PPP2CA/B, $Eng^{-/-}$ cells displayed no TGF-β1-dependent regulation (Fig. 6B). These results indicate that under normal conditions, endoglin prevents the interaction of PP2A with NOS3, regulating NOS3 activation by stimuli such as TGF-β1.

Endoglin Regulates NOS3 Ser1177 Phosphorylation in Endothelial Cells—PP2A is known to dephosphorylate NOS3 at Ser1177. Consistent with NOS/PP2A association increased in the absence of endoglin, we observed that $Eng^{-/-}$ cells displayed lower NOS3 Ser1177 phosphorylation than $Eng^{+/+}$ cells, relative to total NOS3 levels ($p < 0.02$; Fig. 6C). TGF-β1 had no effect on NOS3 Ser1177 phosphorylation in either cell type. Treatment with the PP2A inhibitor, okadaic acid, led to increased NOS3 Ser1177 phosphorylation in $Eng^{+/+}$ cells ($n = 12$ samples/group; 1.6-fold increase, $p < 0.001$) but had no effect in $Eng^{-/-}$ cells given the constitutive dephosphorylation of NOS3 Ser1177 (Fig. 6D). We ruled out any effect of endoglin on AKT mediated phosphorylation of NOS3; the constitutive level of AKT phosphorylation was similar in $Eng^{-/-}$ and $Eng^{+/+}$ cells and in lungs from *Eng* heterozygous *versus* wild type mice respectively (data not shown). These data suggest an important role for endoglin in maintaining

---

cotransfected with pCMV5, Flag-tagged NOS3 and the ACVRL1-HA constructs as indicated, followed by IP with anti-Flag and WB with anti-HA. *D*, Detection of endogenous PP2A/endoglin/eNOS interactions in mouse endothelial cells. Cell lysates were subjected to IP with anti-NOS3 and probed for endoglin, PP2A catalytic subunit (PP2C/A) and NOS3. *E*, Detection of PP2A/ACVRL1/NOS3 complex in mouse endothelial cells. Cell lysates were subjected to IP with control IgG, anti-NOS3 or anti-PP2A-Bβ (to PPP2R2B) and probed for ACVRL1. *F*, Interaction of endoglin with ACVRL1, NOS3 and PP2A in mouse endothelial cells. Lysates were subjected to IP with antibodies to ACVRL1, NOS3, PP2C/A, PP2A/B$\alpha\beta$ (reacting with both PPP2R2A and PPP2R2B), PP2A-Bβ (reacting with PPP2R2B) or control IgG, followed by WB with anti-ENG. *G*, Interaction of NOS3 with PP2A, ACVRL1 and endoglin. Mouse endothelial cell lysates were subjected to IP with antibodies to PP2A/Bα, ACVRL1, and endoglin and probed with anti-NOS3.
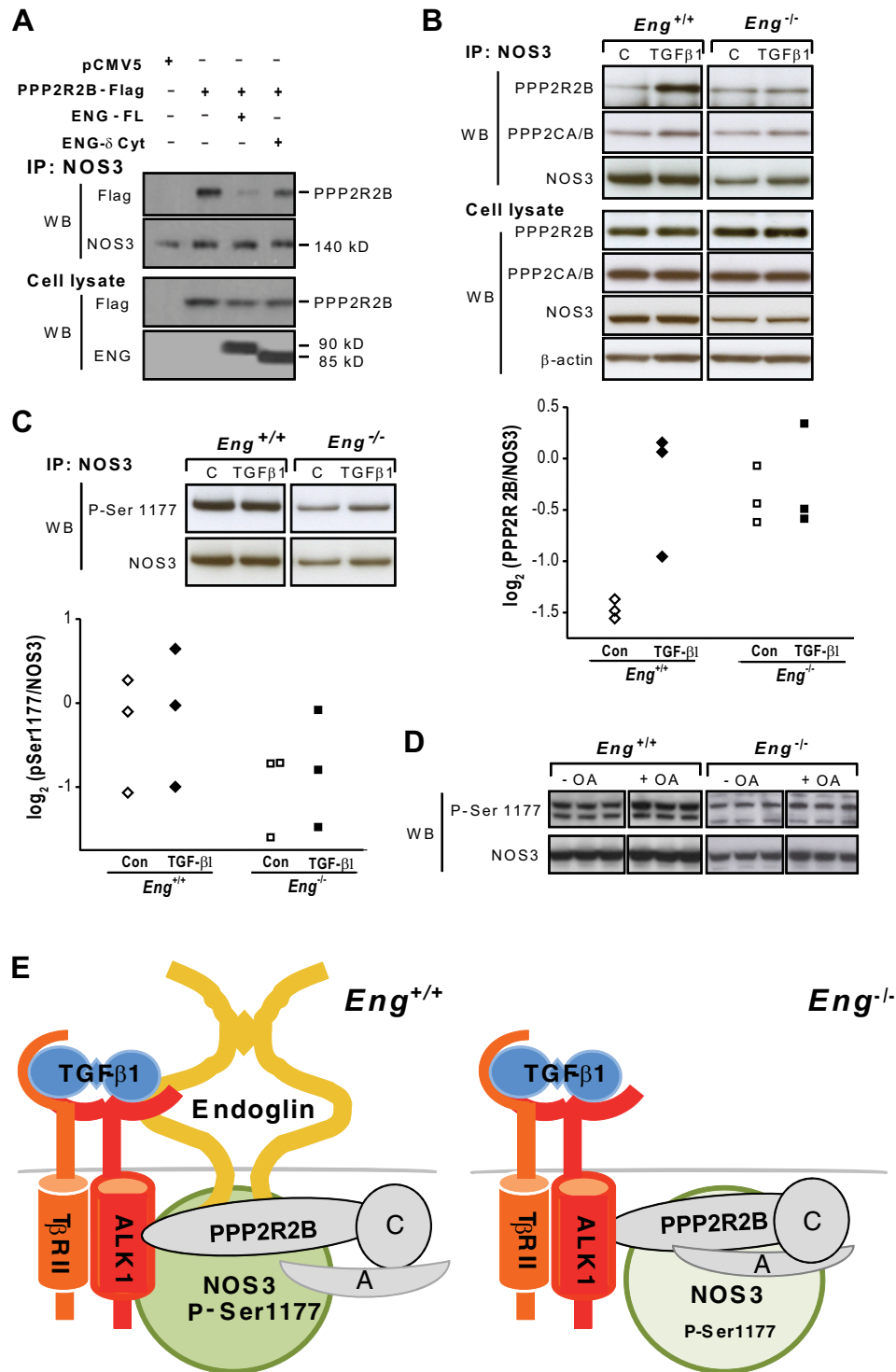
FIG. 6. **Endoglin regulates the interaction of PPP2R2B with NOS3.** *A,* Effects of endoglin on PPP2R2B/eNOS association in bovine endothelial cells. Cells were cotransfected with pCMV5 vector (V), PPP2R2B-Flag, NOS3 and full length ENG (ENG-FL) or cytoplasmic domain-deleted ENG (ENG-δCyt). Total lysates were IP with anti-eNOS, followed by WB with anti-endoglin and anti-Flag; a representative experiment is shown. *B,* Effects of endoglin on PP2A/NOS3 interaction. *Eng*$^{+/+}$ and *Eng*$^{-/-}$ embryonic endothelial cells were treated with vehicle or 10 ng/ml TGF-β1 for 30 min. Lysates were IP using anti-NOS3, followed by WB with antibodies to PP2A-Bβ (PPP2R2B), PPP2CA, or total NOS3. The graph shows the distribution of PPP2R2B-eNOS complex in three experiments. Data expressed as ratios were converted to log$_2$ before 2 × 3 ANOVA analysis. *C,* Effects of endoglin on NOS3-Ser1177 phosphorylation. Cell lysates from *Eng*$^{+/+}$ and *Eng*$^{-/-}$ endothelial cells were IP using anti-NOS3, followed by WB with anti-phospho-NOS3 Ser1177 and anti-NOS3. A representative experiment is shown. The graph illustrates the distribution of phospho-NOS3 Ser1177/total NOS3 complex in 3 experiments. Ratios were converted to log$_2$ before 2 × 3 ANOVA analysis. *D,* Effects of endoglin

basal NOS3 activity, and regulating dephosphorylation at Ser1177 by PP2A following recruitment of the holoenzyme via PPP2R2B (Fig. 6*E*).

DISCUSSION

The LUMIER assay (10, 29) allowed us to test a total of 2052 potential interactions with endoglin, ACVRL1 and TGFBR2 receptors. We identified 191 interactions that passed our stringent criteria, with 181 representing potential novel interactions that may define endothelium-specific and HHT-related effector networks. These previously unrecognized partners might have roles in development, angiogenesis and vascular tone, and when defective could contribute to vascular diseases.

Our data on potential novel interactions and comparison with literature-curated protein interactions allowed us to examine the overlap between the newly defined ACVRL1/TGFBR2/endoglin networks and previously described TGFBR1-dependent networks (10). Many studies have reported a role for membrane endoglin in modulating TGF-β1 and -β3 signaling. Our findings support the concept that endoglin and ACVRL1 (or ALK1) are important components of the TGF-β receptor system in endothelial cells, in a complex that also requires TGFBR1 (ALK5) and TGFBR2.

The novel interactors of ACVRL1, TGFBR2 and endoglin contribute substantially to a serine kinase hub including activin receptors, PAK1 and AKTs. We show that PAK1 interacts with ACVRL1 and endoglin and confirm its interaction with TGFBR2 (10). The p21-activated kinase (PAK) family performs crucial roles during cytoskeletal remodeling, cell migration, and act as downstream effectors of the small GTPases, RAC1, RAC2, and CDC42 (37). RAC2 and ARHGEF6 interacted strongly with ACVRL1. RAC2 is required for postnatal angiogenesis and integrin-dependent migration of endothelial cells (38). ARHGEF6 is a RAC1/CDC42 exchange factor that can activate PAK1. ACVRL1, via its interaction with ARHGEF6, can potentially contribute to the RAC1-PAK1 signaling axis for lamellipodia formation and migration, downstream of AKT in endothelial cells (39).

We identified several novel interactors involved in regulating protein ubiquitylation. FBXO3 and FBXL12 function as adaptors for target recruitment to the Skip-Cul-Fbox (SCF) E3-ubiquitin ligases for proteasomal degradation (40). Both interact with ACVRL1, endoglin and TGFBR2 suggesting that these receptors can be targeted for degradation by SCF complexes. TRIM13, an E3 ubiquitin ligase involved in the retro-translocation and turnover of membrane and secretory proteins from the endoplasmic reticulum (ER) through ER-associated degradation, was found to interact with endoglin. The ubiquitin-binding protein UBXN1, required to couple deglycosylation and proteasome-mediated degradation of misfolded proteins in the ER (41), interacted with endoglin and TGFBR2. The deubiquitylating enzymes include a large group of ubiquitin-specific-proteases (USPs) that counteract the function of ubiquitin E3 ligases; some have been reported to regulate the protein stability of TGF-β pathway members (42). It will be of interest to determine the role of the USPs identified as potential partners for ACVRL1/TGFBR2 (USP21, USP39, and USP45) and for ACVRL1/endoglin (USP16).

We found that ACVRL1 interacts with STUB1, an E3 ubiquitin ligase serving as an adaptor for HSP90, balancing protein folding and degradation (43). Importantly, STUB1 displaces NOS3 from the Golgi, impairing its trafficking to the plasma membrane and activity (44). We speculate that reduced ACVRL1 in HHT may lead to increased NOS3/STUB1 association, which may partly account for the observed dysregulation of NOS3 activation.

A large novel interacting network for endoglin and ACVRL1 identified in this study is centered on the PP2A hub (Fig. 2). Specifically, endoglin, ACVRL1 and TGFBR2 all interact with the regulatory subunit PPP2R2B. We found that endoglin negatively regulates the PPP2R2B/NOS3 interaction and controls the basal level of NOS3 Ser1177 phosphorylation. The *PPP2R2B* gene being a candidate for the HHT3 locus (16, 17), our findings suggest a critical role for the corresponding regulatory subunit in recruiting TGF-β receptors and PP2A to the NOS3 activation complex in endothelial cells, thereby modulating vascular homeostasis.

Several research groups have reported the involvement of PP2A in TGF-β signaling. The regulatory subunit PPP2R2A was shown to associate with TGFBR1 (ALK5), in a reaction potentiated by TGFBR2, causing enhanced TGF-β-dependent growth inhibition (45). We confirmed the interaction of PPP2R2A with TGFBR1, but this regulatory subunit does not appear to associate with ACVRL1. In vertebrates, the PPP2R2A and PPP2R2D subunits were shown to regulate TGF-β/Activin/Nodal signaling in opposite ways (46), PPP2R2A enhancing signals by stabilizing ACVR1B and TGFBR1 basal levels, whereas PPP2R2D restricted receptor activity. Our data imply that the PPP2R2B subunit interacts preferentially with ACVRL1, and independently of its kinase activity, as previously reported for BMPR2 (47). We also confirm that BMPR2 and TGFBR2 associate with PPP2R2B and PPP2R2D. Thus, specific PP2A regulatory subunits may be important in regulating TGF-β superfamily re-

---

on okadaic acid inhibition of NOS3 Ser1177 phosphorylation. Endothelial cells were pretreated with 200 nM okadaic acid (OA) for 90 min and stimulated with vehicle or TGF-β1 for 30 min. *E*, Model illustrating how endoglin regulates NOS3-Ser1177 phosphorylation by PP2A. In endothelial cells, endoglin interacts with TGFBR2 and ACVRL1, but also with NOS3 and PPP2R2B, a regulatory subunit of PP2A. PPP2R2B recruits the TGF-β receptor complex and NOS3 to the A structural and C catalytic subunits of PP2A. In wild-type *Eng*$^{+/+}$ cells, endoglin limits the access of PP2A to NOS3, allowing Ser1177 phosphorylation to remain high, sustaining NO● production. In *Eng*$^{-/-}$ cells, PPP2R2B binds to NOS3 leading to PP2A catalytic subunit-mediated dephosphorylation of Ser1177 residue and impaired NOS3 activity.

---

sponses and PPP2R2B may be particularly critical in endothelial cells as it interacts with both ACVRL1 and endoglin.

Generally, the role of PP2A regulatory subunits is to recruit target proteins to structural and catalytic subunits, leading to either activation or inactivation by dephosphorylating the target proteins. Our data suggest that PPP2R2B interacts with the ACVRL1/TGFBR2/endoglin complex and directs the catalytic subunit of PP2A to NOS3, a process hindered by endoglin. In bovine endothelial cells, endoglin overexpression decreased PPP2R2B/NOS3 association, whereas ENG-δCyt, which cannot interact with intracellular proteins, failed to impair this association. Furthermore, mouse endothelial cells lacking endoglin showed increased amounts of NOS3/PP2A complexes and lower basal NOS3-Ser1177 phosphorylation suggesting that endoglin normally regulates the access of PP2A to NOS3, thereby promoting basal NOS3 activation and NO● production, as illustrated in Fig. 6*E*. In the absence of endoglin, PP2A has more access to NOS3, causing Ser1177 dephosphorylation and compromising its activation.

The activation of NOS3 is highly complex and regulated by dephosphorylation at residue Thr495 and phosphorylation at Ser1177 (25). In endothelial cells, we confirmed that NOS3 Ser1177 (Fig. 6*D*), but not Thr495 (data not shown) phosphorylation, was increased in the presence of the PP2A inhibitor, okadaic acid. The phosphorylation state of NOS3 affects vascular reactivity and Ser1177 phosphorylation can be increased by shear stress and vascular endothelial growth factor (VEGF), leading to NO● production and regulation of vascular tone (48). We previously reported that endoglin and ACVRL1 associate with NOS3 and regulate its activation and NO● production; when cells are deficient in *ENG* or *ACVRL1*, such as in HHT1 and HHT2, NOS3 is in a state of uncoupling, leading to the generation of superoxide rather than NO● (2, 3, 9). Our current observations indicate that endoglin competes with PPP2R2B for binding to NOS3, thereby regulating basal and agonist-induced phosphorylation of this enzyme at Ser1177. The higher level of association between PP2A and NOS3 in *Eng*$^{-/-}$ cells likely contributes to NOS3 dysfunction in HHT. We also show that TGF-β1 stimulates PP2A-NOS3 association in an endoglin-dependent manner. However, our findings suggest an additional role for endoglin in regulating NOS3-Ser1177 phosphorylation via its interaction with PPP2R2B in a TGF-β1-independent manner, and consistent with its high level of expression in endothelial cells.

Our study reports several proteins interacting with endoglin, ACVRL1 and TGFBR2 and focuses on the potential role of the PPP2R2B regulatory subunit in targeting PP2A to the TGF-β receptor complex and NOS3, hereby playing a role in NO● production and vasomotor function. We propose that mutations in the *PPP2R2B* gene may disrupt targeting of PP2A to NOS3, perturbing NOS3 phosphorylation and activation, contributing to endothelial dysfunction and predisposing to HHT and the generation of AVMs. In view of the very low number of families with an apparent HHT3 phenotype, it has been extremely difficult to identify the causative gene and to determine if indeed mutations in the *PPP2R2B* gene give rise to HHT. Such studies would strengthen the role of PP2A in the regulation by endoglin of NOS3 phosphorylation, and activation and control of vascular function and integrity.

¶¶ Correspondence should be addressed to either Michelle Letarte or Mourad Toporsian. Molecular Structure and Function Program, Hospital for Sick Children, 555 University Avenue, Toronto, Ontario, M5G1X8, Canada. Tel.: 416-813-6258; Fax: 416-813-7877; E-mail Michelle.letarte@sickkids.ca. Pulmonary and Critical Care Division, Brigham and Women's Hospital, Harvard Medical School, 20 Shattuck Street Rm-830, Boston, MA 02215. Tel.: 617-278-0763; Fax: 617-264-6873; E-mail: mtopors@partners.org; or E-mail: mtoporsi@gmail.com.

REFERENCES

1. Massague, J., and Gomis, R. R. (2006) The logic of TGFbeta signaling. *FEBS Lett.* **580,** 2811–2820
2. Toporsian, M., Gros, R., Kabir, M. G., Vera, S., Govindaraju, K., Eidelman, D. H., Husain, M., and Letarte, M. (2005) A role for endoglin in coupling eNOS activity and regulating vascular tone revealed in hereditary hemorrhagic telangiectasia. *Circ. Res.* **96,** 684–692
3. Toporsian, M., Jerkic, M., Zhou, Y. Q., Kabir, M. G., Yu, L. X., McIntyre, B. A., Davis, A., Wang, Y. J., Stewart, D. J., Belik, J., Husain, M., Henkelman, M., and Letarte M. (2010) Spontaneous adult-onset pulmonary arterial hypertension attributable to increased endothelial oxidative stress in a murine model of hereditary hemorrhagic telangiectasia. *Arterioscler. Thromb. Vasc. Biol.* **30,** 509–517
4. Shovlin, C. L. (2010) Hereditary haemorrhagic telangiectasia: pathophysiology, diagnosis and treatment. *Blood Rev.* **24,** 203–219
5. Abdalla, S. A., and Letarte, M. (2006) Hereditary haemorrhagic telangiectasia: current views on genetics and mechanisms of disease. *J. Med. Genet.* **43,** 97–110
6. Dimmeler, S., Dernbach, E., and Zeiher, A. M. (2000) Phosphorylation of the endothelial nitric oxide synthase at ser-1177 is required for VEGF-induced endothelial cell migration. *FEBS Lett.* **477,** 258–262
7. Venkatesha, S., Toporsian, M., Lam, C., Hanai, J., Mammoto, T., Kim, Y. M., Bdolah, Y., Lim, K. H., Yuan, H. T., Libermann, T. A., Libermann, T. A., Stillman, I. E., Roberts, D., D'Amore, P. A., Epstein, F. H., Sellke, F. W., Romero, R., Sukhatme, V. P., Letarte, M., and Karumanchi, S. A. (2006) Soluble endoglin contributes to the pathogenesis of preeclampsia. *Nat. Med.* **12,** 642–649
8. Cheifetz, S., Bellon, T., Cales, C., Vera, S., Bernabeu, C., Massague, J., and Letarte, M. (1992) Endoglin is a component of the transforming growth factor-beta receptor system in human endothelial cells. *J. Biol. Chem.* **267,** 19027–19030
9. Jerkic, M., Kabir, M. G., Davies, A., Yu, L. X., McIntyre, B. A., Husain, N. W., Enomoto, M., Sotov, V., Husain, M., Henkelman, M., Belik, J., and Letarte, M. (2011) Pulmonary hypertension in adult Alk1 heterozygous mice due to oxidative stress. *Cardiov. Res.* **92,** 375–384
10. Barrios-Rodiles, M., Brown, K. R., Ozdamar, B., Bose, R., Liu, Z., Donovan,

R. S., Shinjo, F., Liu, Y., Dembowy, J., Taylor, I. W., Luga, V., Przulj, N., Robinson, M., Suzuki, H., Hayashizaki, Y., Jurisica, I., and Wrana, J. L. (2005) High-throughput mapping of a dynamic signaling network in mammalian cells. *Science* **307,** 1621–1625

11. Brown, M. A., Zhao, Q., Baker, K. A., Naik, C., Chen, C., Pukac, L., Singh, M., Tsareva, T., Parice, Y., Mahoney, A., Roschke, V., Sanyal, I., and Choe, S. (2005) Crystal structure of BMP-9 and functional interactions with pro-region and receptors. *J. Biol. Chem.* **280,** 25111–25118

12. David, L., Mallet, C., Mazerbourg, S., Feige, J. J., and Bailly, S. (2007) Identification of BMP9 and BMP10 as functional activators of the orphan activin receptor-like kinase 1 (ALK1) in endothelial cells. *Blood* **109,** 1953–1961

13. Xu, Y., Xing, Y., Chen, Y., Chao, Y., Lin, Z., Fan, E., Yu, J. W., Strack, S., Jeffrey, P. D., and Shi, Y. (2006) Structure of the protein phosphatase 2A holoenzyme. *Cell* **127,** 1239–1251

14. Janssens, V., Longin, S., and Goris, J. (2008) PP2A holoenzyme assembly: in cauda venenum (the sting is in the tail). *Trends Biochem. Sci.* **33,** 113–121

15. Greif, D. M., Kou, R., and Michel, T. (2002) Site-specific dephosphorylation of endothelial nitric oxide synthase by protein phosphatase 2A: evidence for crosstalk between phosphorylation sites. *Biochemistry* **41,** 15845–15853

16. Cole, S. G., Begbie, M. E., Wallace, G. M., and Shovlin, C. L. (2005) A new locus for hereditary haemorrhagic telangiectasia (HHT3) maps to chromosome 5. *J. Med. Genet.* **42,** 577–582

17. Govani, F. S., and Shovlin, C. L. (2010) Fine mapping of the hereditary haemorrhagic telangiectasia (HHT)3 locus on chromosome 5 excludes VE-Cadherin-2, Sprouty4 and other interval genes. *J. Angiogenes Res.* **2,** 15

18. Pece-Barbara, N., Vera, S., Kathirkamathamby, K., Liebner, S., Di Guglielmo, G. M., Dejana, E., Wrana, J. L., and Letarte, M. (2005) Endoglin null endothelial cells proliferate faster and are more responsive to transforming growth factor beta1 with higher affinity receptors and an activated Alk1 pathway. *J. Biol. Chem.* **280,** 27800–27808

19. Kawai, J., Shinagawa, A., Shibata, K., Yoshino, M., Itoh, M., Ishii, Y., Arakawa, T., Hara, A., Fukunishi, Y., Konno, H., Adachi, J., Fukuda, S., Aizawa, K., Izawa, M., Nishi, K., Kiyosawa, H., Kondo, S., Yamanaka, I., Saito, T., Okazaki, Y., Gojobori, T., Bono, H., Kasukawa, T., Saito, R., and Kadota, K. (2001) Functional annotation of a full-length mouse cDNA collection. *Nature* **409,** 685–690

20. Barbara, N. P., Wrana, J. L., and Letarte, M. (1999) Endoglin is an accessory protein that interacts with the signaling receptor complex of multiple members of the transforming growth factor-beta superfamily. *J. Biol. Chem.* **274,** 584–594

21. Malo, N., Hanley, J. A., Cerquozzi, S., Pelletier, J., and Nadon, R. (2006) Statistical practice in high-throughput screening data analysis. *Nat. Biotechnol.* **24,** 167–175

22. Benjamini, Y., and Hochberg, Y. (1995) Controlling the false discovery rate: a practical and powerful approach to multiple testing. *J. R. Stati. Soc. B* **57,** 289–300

23. Turner, B., Razick, S., Turinsky, A. L., Vlasblom, J., Crowdy, E. K., Cho, E., Morrison, K., Donaldson, I. M., and Wodak, S. J. (2010). iRefWeb: interactive analysis of consolidated protein interaction data and their supporting evidence. *Database : J. Biol. Databases Curation* **2010,** baq023

24. Chatr-Aryamontri, A., Breitkreutz, B. J., Heinicke, S., Boucher, L., Winter, A., Stark, C., Nixon, J., Ramage, L., Kolas, N., O'Donnell, L., Reguly, T., Breitkreutz, A., Sellam, A., Chen, D., Chang, C., Rust, J., Livstone, M., Oughtred, R., Dolinski, K. and Tyers, M. (2013) The BioGRID interaction database: 2013 update. *Nucleic Acids Res.* **41,** D816–D823

25. Dudzinski, D. M., Igarashi, J., Greif, D., and Michel, T. (2006) The regulation and pharmacology of endothelial nitric oxide synthase. *Annu. Rev. Pharmacol. Toxicol.* **46,** 235–276

26. Lee, N. Y., Golzio, C., Gatza, C. E., Sharma, A., Katsanis, N., and Blobe, G. C. (2012) Endoglin regulates PI3-kinase/Akt trafficking and signaling to alter endothelial capillary stability during angiogenesis. *Mol. Biol. Cell* **23,** 2412–2423

27. Vilella, A. J., Severin, J., Ureta-Vidal, A., Heng, L., Durbin, R., and Birney, E. (2009) EnsemblCompara GeneTrees: Complete, duplication-aware phylogenetic trees in vertebrates. *Genome Res.* **19,** 327–335

28. Ostlund, G., Schmitt, T., Forslund, K., Kostler, T., Messina, D. N., Roopra, S., Frings, O., and Sonnhammer, E. L. (2010) InParanoid 7: new algorithms and tools for eukaryotic orthology analysis. *Nucleic Acids Res.* **38,** D196–D203

29. Miller, B. W., Lau, G., Grouios, C., Mollica, E., Barrios-Rodiles, M., Liu, Y., Datti, A., Morris, Q., Wrana, J. L., and Attisano, L. (2009) Application of an integrated physical and functional screening approach to identify inhibitors of the Wnt pathway. *Mol. Syst. Biol.* **5,** 315

30. Guerrero-Esteo, M., Sanchez-Elsner, T., Letamendia, A., and Bernabeu, C. (2002) Extracellular and cytoplasmic domains of endoglin interact with the transforming growth factor-β receptors I and II. *J. Biol. Chem.* **277,** 29197–29209

31. Kawabata, M., Chytil, A., and Moses, H. L. (1995) Cloning of a novel type II serine/threonine kinase receptor through interaction with the type I transforming growth factor-beta receptor. *J. Biol. Chem.* **270,** 5625–5630

32. Vitullo, J. C., Mekhail, N. A., Estafanous, F. G., Khairallah, P. A., and Engelmann, G. L. (1993) Acute morphological effects of cocaine on rat cardiomyocytes. *Cytobios* **76,** 31–39

33. Yao, D., Ehrlich, M., Henis, Y. I., and Leof, E. B. (2002) Transforming growth factor-beta receptors interact with AP2 by direct binding to beta2 subunit. *Mol. Biol. Cell* **13,** 4001–4012

34. Sanz-Rodriguez, F., Guerrero-Esteo, M., Botella, L. M., Banville, D., Vary, C. P., and Bernabeu, C. (2004) Endoglin regulates cytoskeletal organization through binding to ZRP-1, a member of the LIM family of proteins. *J. Biol. Chem.* **279,** 32858–32868

35. Datta, P. K., Chytil, A., Gorska, A. E., and Moses, H. L. (1998) Identification of STRAP, a novel WD domain protein in transforming growth factor-beta signaling. *J. Biol. Chem.* **273,** 34671–34674

36. Goumans, M. J., Valdimarsdottir, G., Itoh, S., Lebrin, F., Larsson, J., Mummery, C., Karlsson, S., and ten Dijke, P. (2003). Activin receptor-like kinase (ALK)1 is an antagonistic mediator of lateral TGFbeta/ALK5 signaling. *Mol. Cell* **12,** 817–828

37. Kichina, J. V., Goc, A., Al-Husein, B., Somanath, P. R., and Kandel, E. S. (2010) PAK1 as a therapeutic target. *Expert Opin Ther Targets* **14,** 703–725

38. De, P., Peng, Q., Traktuev, D. O., Li, W., Yoder, M. C., March, K. L., and Durden, D. L. (2009) Expression of RAC2 in endothelial cells is required for the postnatal neovascular response. *Exp. Cell Res.* **315,** 248–263

39. Somanath, P. R., and Byzova, T. V. (2009) 14–3-3beta-Rac1-p21 activated kinase signaling regulates Akt1-mediated cytoskeletal organization, lamellipodia formation and fibronectin matrix assembly. *J. Cell. Physiol.* **218,** 394–404

40. Postow, L., and Funabiki, H. (2013) An SCF complex containing Fbxl12 mediates DNA damage-induced Ku80 ubiquitylation. *Cell Cycle* **12,** 587–595

41. Wu-Baer, F., Ludwig, T., and Baer, R. (2010) The UBXN1 protein associates with autoubiquitinated forms of the BRCA1 tumor suppressor and inhibits its enzymatic function. *Mol. Cell. Biol.* **30,** 2787–2798

42. De Boeck, M., and ten Dijke, P. (2012) Key role for ubiquitin protein modification in TGFbeta signal transduction. *Ups J. Med. Sci.* **117,** 153–165

43. Muller, P., Ruckova, E., Halada, P., Coates, P.J., Hrstka, R., Lane, D. P., and Vojtesek, B. (2013) C-terminal phosphorylation of Hsp70 and Hsp90 regulates alternate binding to co-chaperones CHIP and HOP to determine cellular protein folding/degradation balances. *Oncogene* **32,** 3101–3110

44. Jiang, J., Cyr, D., Babbitt, R. W., Sessa, W. C., and Patterson, C. (2003) Chaperone-dependent regulation of endothelial nitric-oxide synthase intracellular trafficking by the co-chaperone/ubiquitin ligase CHIP. *J. Biol. Chem.* **278,** 49332–49341

45. Griswold-Prenner, I., Kamibayashi, C., Maruoka, E. M., Mumby, M. C., and Derynck, R. (1998) Physical and functional interactions between type I transforming growth factor beta receptors and Balpha, a WD-40 repeat subunit of phosphatase 2A. *Mol. Cell. Biol.* **18,** 6595–6604

46. Batut, J., Schmierer, B., Cao, J., Raftery, L. A., Hill, C. S., and Howell, M. (2008) Two highly related regulatory subunits of PP2A exert opposite effects on TGF-beta/Activin/Nodal signalling. *Development* **135,** 2927–2937

47. Bengtsson, L., Schwappacher, R., Roth, M., Boergermann, J. H., Hassel, S., and Knaus, P. (2009) PP2A regulates BMP signalling by interacting with BMP receptor complexes and by dephosphorylating both the C-terminus and the linker region of Smad1. *J. Cell Sci.* **122,** 1248–1257

48. Scotland, R. S., Morales-Ruiz, M., Chen, Y., Yu, J., Rudic, R. D., Fulton, D., Gratton, J. P., and Sessa, W. C. (2002) Functional reconstitution of endothelial nitric oxide synthase reveals the importance of serine 1179 in endothelium-dependent vasomotion. *Circ. Res.* **90,** 904–910